Journal of Materials Chemistry C

RSC Publishing

PAPER

View Article Online
View Journal | View Issue

Dichroic-dye-doped polymer stabilized optically isotropic chiral liquid crystals

Cite this: *J. Mater. Chem. C*, 2013, **1**, 6471

Zhi-gang Zheng,*[ab] Chao Wang[a] and Dong Shen*[a]

A polarization-independent electro-optical material based on dichroic-dye-doped polymer stabilized optically isotropic chiral liquid crystals is prepared. The isotropic phase of the material can be well maintained even though the temperature is below 0 °C. The electro-optical performances of the material are explored, and the results show large Kerr constant ($K \sim 10$ nm V^{-2}), fast response time (only hundreds of microseconds), and large contrast ratio (nearly 9.0). It can be estimated that the power consumption and the cost of the devices based on this material can be decreased substantially, due to the alignment-free and polarizer-free characteristics. Therefore, this material will be a good candidate in the next-generation low power consumption displays and other photonic devices.

Received 29th May 2013
Accepted 14th August 2013

DOI: 10.1039/c3tc31013b

www.rsc.org/MaterialsC

Introduction

Optically isotropic liquid crystals (OILCs) have attracted much attention recently because of their advantages of polarization-independence, alignment-free and fast response.[1] Currently, researchers are most interested in two typical OILCs, one is blue phase (BP), the other is optically isotropic chiral liquid crystal (OICLC). BP is a special LC phase with a double twisted arrangement. The helical axes cross each other and form a double twisted cylinder (DTC). Usually, BP has three sub-phases with DTCs uniformly distributed: fog-like BPIII, or self-assembled cubic BPII and I. All of the three sub-phases are optically isotropic.[2,3] In recent years, many efforts have been made to overcome some shortcomings of BPs. To extend the BP range, many kinds of methodology have been proposed, such as polymer stabilization,[4] designing and synthesizing bimesogen[5] or T-shaped LCs,[6] and doping with bent-shaped molecules[7] or nanoparticles.[8] Among these wide BP range materials, polymer stabilized blue phases (PSBPs) are more favorable because of their stable properties, however the hysteresis and high driving voltage are two troublesome problems. To improve them, some new PSBP composites with good performance were developed.[9–12] Besides, a variety of devices for display and photonic applications were also fabricated.[13–18]

OICLCs, which were reported by Kikuchi *et al.*,[19] have similar optical properties as BPs, but their textures are different. Because the CLC domain size is smaller than the wavelength of visible light, the colorful platelets of BP are replaced by a dark state of OICLC. Similarly, a polymer stabilization technique is also adopted to expand the isotropic temperature range of such materials, giving so-called polymer stabilized optically isotropic chiral liquid crystals (abbreviated as PS-OICLC).[20] Such PS-OICLCs can be obtained by UV-exposure of the sample at an isotropic phase (above the clearing point). The driving mode for PS-OICLCs is the same as that for PSBPs, in-plane switching (IPS). However as reported, the driving voltage is low and the Kerr constant is large for PS-OICLCs.[21] From the display point of view, PS-OICLCs possess similar advantages to PSBP, such as free alignment, sub-millisecond response time, wide viewing angle and cell gap insensitivity.[1] Besides, the light leakage of PSBP in the voltage-off state can be suppressed by utilizing PS-OICLC, thus the contrast ratio (CR) is expected to be improved further.

For the purpose of displays, whether we use PSBP or PS-OICLC, the polarizer is still necessary for the IPS mode, thus the optical efficiency of the device would be reduced. To solve this problem, and inspired by the principle of guest–host display mode, Lin *et al.* fabricated a polarization-independent (polarizer-free) PSBP display by doping a small amount of black dichroic dye into the PSBP system.[22] The BP could stably exist in the range from 20 to 40 °C; the sample could be voltage-tuned between black and transparent; and the response time was 5.16 ms. Moreover, to improve the CR of the device, the reflection mode was selected to double the optical path and enhance the absorption in the voltage-off state, so that the CR was increased to 3.23 : 1.

In this work, a kind of dichroic-dye doped PS-OICLC is fabricated. Unlike the above reported work, we herein synthesize a kind of azo-based dye with high dichroism as the dopant. The absorption band of this dye lies in the visible range, from 400 to 500 nm, therefore the whole dye-doped mixture is red in macro-scale in the voltage-off state. We consider that such a

[a]*Department of Physics, East China University of Science and Technology, No.130, Meilong Road, Shanghai, 200237, China. E-mail: zgzheng@ecust.edu.cn; shen@ecust.edu.cn; Fax: +86-21-64253514; Tel: +86-21-64253514*

[b]*National Laboratory of Solid State Microstructures and College of Engineering and Applied Sciences, Nanjing University, Nanjing 210093, China*

material may be promising in low power consumption displays or other photonic devices. In the following parts, the materials and testing methods are given; the performances of this material, such as CR, polarization-independence, hysteresis, response time, and Kerr effect, are tested and compared with those of published results; in addition, the tested results are discussed from the materials chemistry and physics points of view; in the last part, we give the conclusions.

Materials and testing methods

Materials used in our experiments are mainly composed of the chiral nematic liquid crystals (N*LCs) and a small amount of photopolymerizable monomers with the weight ratio of 93 : 7. The N*LCs are prepared using the commercial NLC host (XH-07X supplied by Xianhua Chemical Co., Ltd., China. $\Delta n = 0.169$ @ 532 nm, and clearing point is 62.4 °C) and the chiral agent R811 (supported by Merck) with the weight ratio of 3 : 1. The monomers are mixed with two kinds of acrylate-based materials, one is 2-EHA (2-ethylhexyl acrylate), the other is $PTPTP_n$ which is composed of two similar materials, $PTPTP_3$ and $PTPTP_6$, with weight ratio 1 : 1. The chemical structure of $PTPTP_n$ has been reported in detail previously.[23,24] The weight ratio of 2-EHA and $PTPTP_n$ is 1 : 2.

The azo-based dichroic dye is synthesized according to the routes depicted in Scheme 1. The dye is obtained as a red solid, and its chemical structure is shown in Fig. 1(a). ^{1}H NMR ($CDCl_3$, 400 MHz): δ(ppm) 1.00(t, J = 7.36 Hz, 3H, –CH_3), 1.53(m, 2H, –CH_2–), 1.68–1.72(m, 6H, –CH_2–), 1.82(m, 2H, –CH_2–), 3.39(t, J = 5.44 Hz, 4H, –CH_2–), 4.06(t, J = 6.52 Hz, 2H, –CH_2–), 6.96–7.03(m, 4H, Ar–H), 7.88–8.01(m, 8H, Ar–H). MS (ESI+) m/z 441.25 $[M + H]^+$.

By doping the dye carefully into the N*LC–monomer mixture, and varying the concentration from 0.75 to 1.75 wt% with a step of 0.25 wt%, five samples can be prepared for comparison and optimization of the mixing ratio. The samples are sequentially labeled as Sample A, B, C, D and E for convenience. In addition, about 0.5 wt% photoinitiator (Irgacure 184, BASF) are mixed in the material systems for photopolymerization. The contents of these samples are given in Table 1. The mixtures are uniformly stirred at the temperature of 60 °C (about 10 °C higher than the clearing point) for 24 hours, and then injected by capillarity into 15 μm thick cells with planar ITO electrodes. The samples are set on a precisely

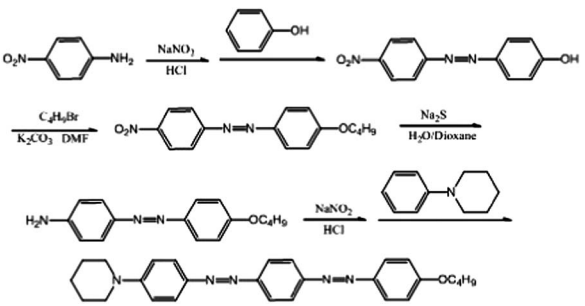

Scheme 1 Synthetic route to the azo dye used in this work.

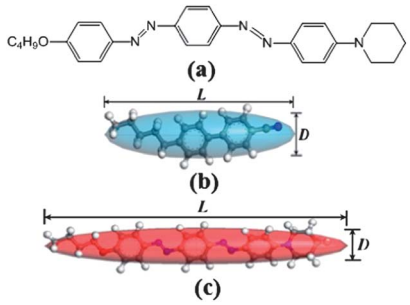

Fig. 1 The chemical structure of the dichroic dye (a); atomistic models of 5CB (b) and the dichroic dye (c).

controlled hot-stage (Instec HCS-302) and maintained at the temperature of 5 °C above the clearing point for about 1 hour. As the whole material system reaches thermal equilibrium, it is exposed for stabilizing the isotropic phase. In our experiment, 365 nm UV is selected as the exposure source (the selection of UV source seems unreasonable. However we consider it is suitable on the basis of our following experimental results. We will discuss it in the next part), and the intensity is modulated to 2.0 mW cm^{-2}, the exposure time for each sample is 40 minutes.

The temperature range of isotropic phase is evaluated using the hot-stage at the cooling rate of 0.5 °C min^{-1}. The optical and electrically tunable properties of the samples are tested by an optical-fiber-connected microscope. As shown in Fig. 2, the backlight of the microscope is used as the white-light source. The light transmits through the sample and impinges on a dual-channel fiber adaptor. Such an adaptor can split the incident light into two beams, one is received by spectroscope for the spectral analysis, the other is detected by an oscilloscope-connected photoelectric converter for response analysis. A 1 kHz voltage signal is applied through the signal generator, so the electrically tunable performances can be tested. The property of polarization independence can be tested by setting a polarizer on the holder and rotating it to change the polarization direction of the incident light. The sample is placed on the microscope stage and tested at room temperature (about 18 °C).

The Kerr constant (K) of the optically isotropic material is also tested using the following theoretical expression,

$$\Delta n = \lambda K E^2 \quad (1)$$

Eqn (1) indicates that electric-field-induced birefringence (Δn) is proportional to the square of the electric field (E), as the

Table 1 Content (wt%) of the dye-doped polymer-stabilized optically isotropic liquid crystals

Sample	NLC	R811	EHA	$PTPTP_n$	Dye	Photoinitiator
A	68.06	22.69	2.67	5.33	0.75	0.5
B	67.88	22.62	2.67	5.33	1.00	0.5
C	67.69	22.56	2.67	5.33	1.25	0.5
D	67.50	22.50	2.67	5.33	1.50	0.5
E	67.31	22.44	2.67	5.33	1.75	0.5

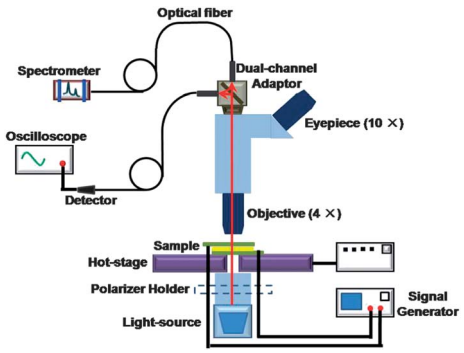

Fig. 2 Testing setup in the experiment.

wavelength (λ) of the light source is constant. Therefore K can be obtained by calculating the slope of the line (Δn–E^2). The electric-field dependent birefringence of the sample is tested through the conventional Senarmont method.[23,25] However, the IPS driving mode always leads to a non-uniform distribution of electric field in the cell, which will bring about some testing errors of the Kerr constant.[19,23] Considering this aspect, planar ITO cells are selected to generate a uniform electric field for the testing. It is noteworthy that the testing beam needs to be obliquely incident on the cell (the incident angle is defined as θ), thus the change of Δn under the applied field can be detected. The Δn–E^2 curve at a certain incidence angle (θ) can be obtained, and the extended Kerr equation is used to fit this curve,[25,26] thus the incidence angle related Kerr constant, K_θ, is calculated. Next, testing the K_θ at other θ values according to the method mentioned above, an equation of θ *versus* K can be fitted using the θ–K data. As we substitute $\theta = 90°$ into the equation, the Kerr constant independent of the distribution of electric field is calculated. Some details of Kerr constant testing can also be found in ref. 23, 25 and 26.

Results and discussion

Properties of dichroic dye

Before the preparation of PS-OICLC samples, the properties of the dichroic dye should be studied. The phase sequence is tested by differential thermal analyser (DTA) and then rechecked through the polarized optical microscope (POM). The results show that the crystalline phase is retained at temperatures below 249 °C. When the temperature reaches 249 °C, the crystal transforms to the fluid phase with thread-like disclination lines (as shown in Fig. 3(b)), that is the typical nematic phase which can be maintained between 249 and 273 °C. The nematic phase transforms to the isotropic phase at the clearing point, 273 °C (as shown in Fig. 3(c)).

A small amount of dye (~1.75 wt%) is doped into the NLC host mentioned above (dye-doped NLC) and injected into a parallel aligned cell to form the homogeneous orientation, and then the transmission spectral characteristics can be tested. As shown in Fig. 4, an evident absorption band, range from 400–500 nm, can be observed, and such absorption is caused by the azo chromophore in the dye molecules. As a voltage is applied to the cell, the absorbance decreases gradually because of the reorientation of dichroic dyes with the rotation of LCs under the electric field. Fig. 4 shows that when the voltage is large enough, *e.g.* saturation voltage, the transmittance increases from 2.2–2.5% to 42–45%. In addition, the absorption coefficients ($\alpha_\parallel$ and $\alpha_\perp$) and the dichroism ($\Delta\alpha = \alpha_\parallel - \alpha_\perp$) of the dye can be calculated through Beer's law,[27]

$$I_T = I_0 e^{-c\alpha l} \quad (2)$$

in which I_0 and I_T are the intensity before and after the light transmits through the sample; c and α are the content and the absorption coefficient of dichroic dye respectively; and l is the cell gap. Combining with the transmission spectrum shown in Fig. 4, the light intensity can be calculated by integrating the area of the spectrum from 400 to 500 nm; c and l can be substituted directly in eqn (2). In the OFF state (green spectrum in Fig. 4), the absorption coefficient of the sample is defined as $\alpha_\parallel$; as the saturation voltage is applied on the sample (blue spectrum in Fig. 4), the absorption coefficient is $\alpha_\perp$. Thus, the calculated absorption coefficients are $\alpha_\parallel = 34.4\ \mu m^{-1}$, $\alpha_\perp = 9.1\ \mu m^{-1}$; and the dichroism of the dye is $\Delta\alpha = 25.3\ \mu m^{-1}$, which is much larger than that reported in the previous work.[22]

The UV-Visible absorption spectrum of the dye is detected, and two peaks at 365 and 452 nm are found in Fig. 5, which correspond to the *trans*-to-*cis* and *cis*-to-*trans* isomerizations. As mentioned before, 365 nm UV is used as the irradiation source to carry out the photopolymerization of monomer and form the PS-OICLC samples. However, would the UV-induced isomerization of the dyes affect the stabilization and the optical performances of the sample? To clarify this issue, a small amount of the dye is dissolved into the NLC host and injected into the quartz cell, and then exposed to the 365 nm UV source

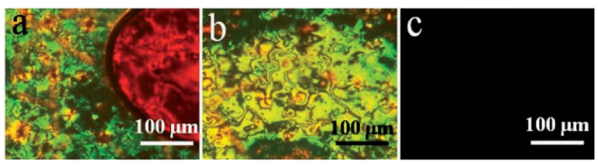

Fig. 3 Micrographs and phase transition temperatures of dichroic-dye. Cryst–N @ 249 °C (a), N @ 260 °C (b), Iso @ 273 °C (c).

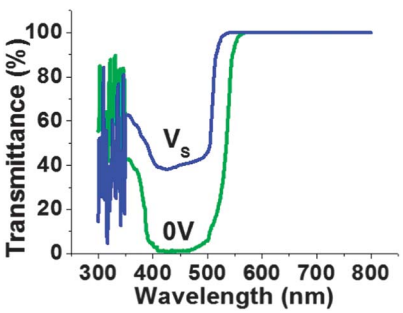

Fig. 4 Voltage modulated transmission spectrum (homogeneous aligned cell). Blue line is the transmission spectrum at $V = V_S$, green line is the transmission spectrum in the absence of applied voltage.

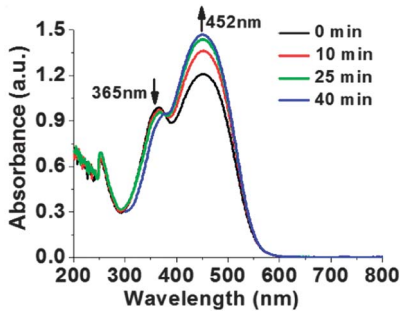

Fig. 5 The UV absorption behaviour of the dichroic dye during UV exposure.

with the same intensity as is used for polymerization. The UV-Visible spectra are recorded during the process of exposure. As shown in Fig. 5, the peak at 365 nm drops while the other peak at 452 nm rises with the extension of exposure time, but their changes are very small. Such results indicate that there is little influence of UV exposure on the isomerization. In addition, the large temperature range (low-limit temperature is below 0 °C) of the dye-doped PS-OICLC also shows a good stabilization of the sample. Besides, considering the solubility of the photoinitiator with the NLCs and the higher initiated efficiency of the UV source, the selection of 365 nm UV is more reasonable.

Performances of the dye-doped PS-OICLC

The voltage dependent CR of the samples listed in Table 1 is tested to compare the electro-optical (E-O) performance of the samples. The CR herein is defined as the integral area ratio of the transmission spectral range from 400 to 500 nm between the voltage on and off states. The backlight of microscope is used as the unpolarized source.

As shown in Fig. 6, CR increases with the increasing of applied voltage because of the rotation of dyes with the LCs and saturates as the voltage reaches about 70 V_{rms}. In addition, like all other dichroic-dye-doped systems, the saturation CR rises with the increasing of dye content. As the content increases to 1.75 wt%, CR rises to 8.9, which is almost twice as large as that of the dichroic-dye-doped PSBP reported previously,[22] because of the higher dichroism of the dye used herein. However, if the dye content continually increases, no evident rising can be found. The reason for that may lie in the lower solubility of the dye in the N*LC–monomer mixture. To confirm this, the melting points of mixtures with different amounts of dyes are tested. The results show that the melting point rises for about 15 °C as the dye content increases from 0 to 1.75 wt%, which is caused by the solution of the dyes; however no evident increase is shown as the dye content exceeds 1.75 wt%. Actually, we also find lots of undissolved red particles (inset of Fig. 6) in the mixtures with 2 or 3 wt% dyes by using a microscope, which indicates the solubility limit of the dye is only about 1.75 wt%. The saturation voltage is also compared in Fig. 6, it is almost unchanged with the doping of the dye.

The theoretical saturation CR can also be calculated through the absorption coefficients ($\alpha_{\parallel}$ and $\alpha_{\perp}$). However, the α of PS-OICLC in the voltage-off state should be expressed as ($\alpha_{\parallel}$ + $2\alpha_{\perp}$)/3, thus, the saturation CR can be calculated as follows,

$$CR = \frac{I_{ON}}{I_{OFF}} = e^{\frac{\Delta\alpha}{3}cl} \quad (3)$$

The calculated CR of sample E (1.75 wt% dye) is approximately 9.1, which is slightly larger than the tested value, 8.9. Thus, we investigate the order parameter (S) of the dyes in PS-OICLC (dye-doped PS-OICLC system), under the condition that a saturation voltage is applied. The relationship between S and absorption coefficients ($\alpha_{\parallel}$ and $\alpha_{\perp}$) can be expressed by eqn (4),[22]

$$S = \frac{\alpha_{\parallel}/\alpha_{\perp} - 1}{\alpha_{\parallel}/\alpha_{\perp} + 2} \quad (4)$$

We calculate the order parameter of dyes in the NLC host (dye-doped NLC system; 1.75 wt% dye content) by substituting $\alpha_{\parallel}$ = 34.4 μm^{-1} and $\alpha_{\perp}$ = 9.1 μm^{-1} into eqn (4), and S = 0.48. The low value of S might be caused by the weak interaction between the dye molecules and the NLCs. To explore the order parameter of dyes in PS-OICLC systems, $\alpha_{\parallel}$ and $\alpha_{\perp}$ in such dye-doped PS-OICLCs are calculated by using eqn (2) and (3) and the tested intensity of the incident beam (I_0) and the transmitted beam (I_T). Then, order parameter of the dyes can be obtained by substituting the absorption coefficients into eqn (4). As Fig. 7(a) shows, S monotonously increases with the applied voltage and gradually reaches saturation near 70 V, which coincides with the trend presented in Fig. 6. When the applied voltage is 80 V, S is calculated as 0.47, only 0.01 lower than that of dye-doped NLCs. Such results indicate that, as the saturation voltage is applied, the orientation of dyes and LCs in dye-doped PS-OICLC systems

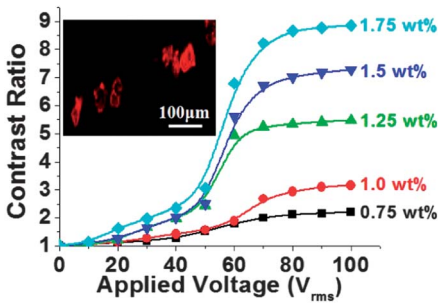

Fig. 6 The voltage-dependent CR of the samples with the increasing of the dye content. Inset: POM photograph of the N*LC–monomer mixture with 2 wt% dye (texture at the temperature above the clearing point).

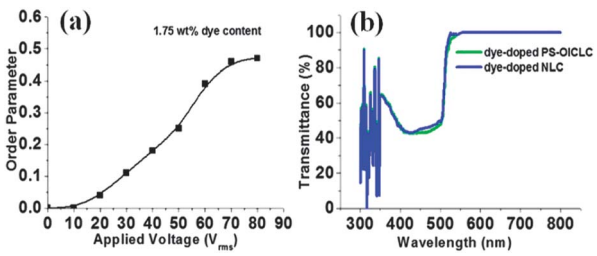

Fig. 7 Voltage-dependent S of 1.75 wt% dye-doped PS-OICLC (a); spectra of the dye-doped PS-OICLC (green line) and dye-doped NLC (blue line) as a saturation voltage is applied (b), dye content is 1.75 wt%.

is almost the same as that in dye-doped NLCs. As a saturation voltage is applied on the sample, the transmission spectra of dye-doped PS-OICLC and dye-doped NLC are tested and shown in Fig. 7(b). The two spectra nearly coincide with each other apart from a little reduction of transmission for the dye-doped PS-OICLC; such results further proves the similar orientation of dyes in the two systems as a saturation voltage is applied. The reason for the lower transmission of dye-doped PS-OICLC is supposed to be related with the binding of polymer network to the dyes, which prevents the rotation of dyes under the applied electric field. Also for this reason, the calculated CR is slightly larger than the tested value. To improve CR further, some methodologies, such as increasing the dichroism ($\Delta\alpha$) and the content (c) of the dye, as well as the cell gap (l), may be feasible ways according to the expression of eqn (3). In addition, using the reflection mode to double the optical path is also very effective.

Considering the solubility limitation of dyes, we further explore the relationship of order parameter (S) of the dye with the dye content. As shown in Fig. 8, S slightly decreases with the increasing of the dye content. When the dye content is low (<1.0 wt%), S is about 0.53. Continually doping the dye, S decreases from 0.53 to 0.47, and reaches the saturation as the content exceeds 1.75 wt%, the solubility limit. Therefore, although increasing the dye content is helpful for enhancing the absorbance of the PS-OICLC and improving the contrast ratio, it also leads to the reduction of order parameter of the dye which in turn affects the contrast ratio.

Subsequently, to make sure of the polarization independence, a polarizer is settled in the "holder" position (shown in Fig. 2) and rotated to change the polarization direction of the incident light. Meanwhile, the voltage-dependent CR curves at 0°, 45° and 90° polarization directions (0° herein is defined as the direction parallel to the x-axis of the conventional Cartesian coordinate system) are tested and shown in Fig. 9. The three curves almost coincide, which proves the polarization independence of the material.

The polymer-stabilized LC systems often exhibit memory effects, known as hysteresis. Large hysteresis always leads to many problems during electrical modulation,[28,29] and hence a smaller or no hysteresis material is preferred. We test the hysteresis of the samples. Fig. 10 shows the hysteresis behaviour for the samples with different dye contents. The result

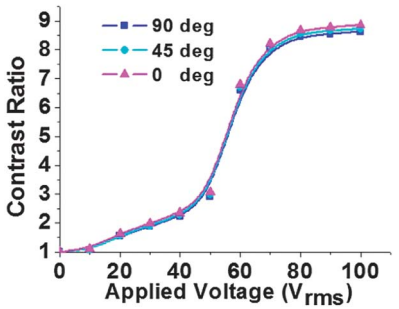

Fig. 9 Voltage-dependent CR behaviour as the polarization directions are 0°, 45° and 90°.

obviously shows that hysteresis is enhanced with the increasing of dye content. This result may be related with the increasing of the interaction between dye molecules, which leads to more time for the LCs to reorient the dyes with the electric field.

The response times of samples A–E (as shown in Table 1) are tested at room temperature (about 20 °C) by applying 80 V voltage. As shown in Fig. 11(a), the rise and decay times are extended with the increasing of the dye. When the dye content is 0.75 wt%, the rise and decay times are 324 and 480 μs, respectively; as this content reaches 1.75 wt%, the corresponding times extend to about 600 and 750 μs, respectively. In addition, we also find that the response time is linearly dependent on the dye content. The reason is considered to be the influence of dye content on the visco-elastic coefficient (γ/K) of the system. As conventional guest–host devices, γ/K increases linearly with the increasing of dye content.[30] The response time can be expressed as,[30,31]

$$\tau = \frac{\gamma}{K}\frac{P^2}{(2\pi)^2} \quad (5)$$

The pitch is independent of the dye content, thus the response time (τ) is determined by γ/K, and shows a similar linear tendency. In addition, as mentioned in ref. 22, in the dye-doped PSBP system, a two-step response can be found. The first step, with a short response time, corresponds to the reorientation of dyes brought about by the rotation of LCs, and the second step corresponds to the distortion of the BP lattice which normally needs a long time, more than 1 ms as reported. However, such a phenomenon is not found in our experiment. As shown in

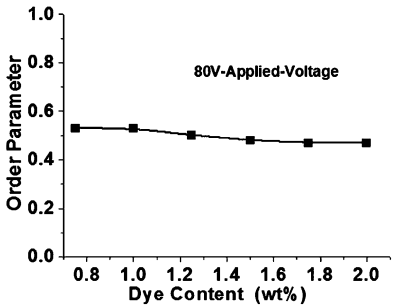

Fig. 8 Order parameter of dyes in PS-OICLC with different dye contents.

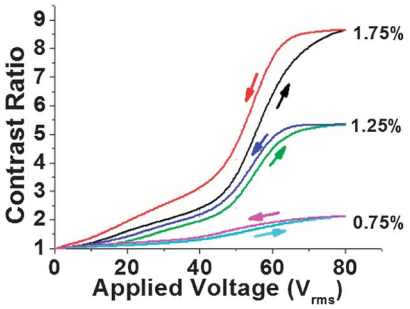

Fig. 10 Hysteresis of dye-doped PS-OICLCs with 0.75, 1.25, and 1.75 wt% dye.

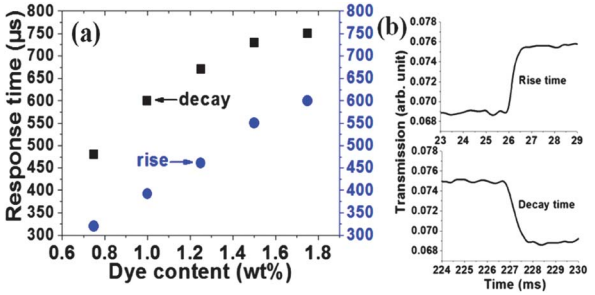

Fig. 11 The rise and decay times for the dye-doped PS-OICLCs with different dye contents (a); the measured rise time and decay times for sample E, with 1.75 wt% dyes (b).

Fig. 11(b), only a one-step response appears for both the rise and decay processes. The reasons may lie in the following aspects: (a) unlike the PSBP, there is no cubic structure in PS-OICLC, thus no lattice distortion but the local unwinding of the CLC to a homeotropic state. Results reported in ref. 21 also prove this; (b) comparing with the PSBP reported in ref. 22, the helical pitch of the PS-OICLC is supposed to be smaller (the size of the domain is much smaller than the wavelength because of its optical isotropy), besides, the polymer concentration is also higher; these two points result in the one-step and faster response for PS-OICLC. Therefore, the response time of dye-doped PS-OICLC is much faster than that of dye-doped PSBP.

For an optically isotropic material, the Kerr effect is an important property that reflects the electro-optical behaviour of devices. The Kerr constant is normally used to evaluate the Kerr effect of a sample. Fig. 12 gives the tested Kerr constants and shows large values (>10 nm V^{-2}) for all of the samples. As discussed in the previous works, such an evident Kerr effect can be ascribed to the easier reorientation of CLC domains under the low electric field.[19] Besides, the large pseudo-CLC domain, *i.e.* large coherent length, is the other main reason for a large Kerr constant; and the polymer network in the system also suppresses the electric-field-induced phase transition from isotropic to LC phase. Comparing the experimental results, the Kerr constants of the samples are several times larger than the reported ones.[19,21] According to the equation of the Kerr constant,[32,33]

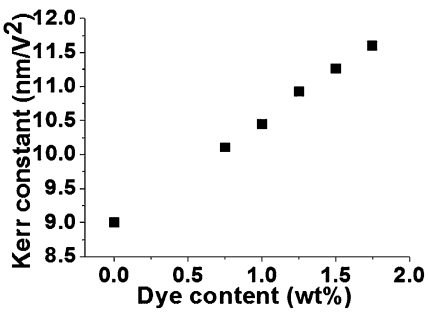

Fig. 12 Kerr constants of the dye-doped PS-OICLCs with different dye contents. Tested at 18 °C, wavelength of the testing source is 532 nm.

$$K \approx \Delta n \cdot \Delta\varepsilon \frac{\varepsilon_0 P^2}{k\lambda(2\pi)^2} = \frac{\Delta n}{\lambda E_S{}^2} \quad (6)$$

in which Δn and $\Delta\varepsilon$ are the electric-field-induced birefringence and dielectric constant; k and P are the elastic constant and the pitch of CLC, respectively; λ is the wavelength of the light source which is defined as before (532 nm laser is the testing source); ε_0 is the permittivity in vacuum; and E_S is the saturation electric field. The reasons for the large Kerr constant can be qualitatively analyzed from three aspects: (a) $\Delta\varepsilon$ of the NLCs host used in the experiment is tested as 33.3, which is three to six times those of the NLCs (5CB $\Delta\varepsilon = 11.5$ and JC-1041 $\Delta\varepsilon = 5.5$) used in the reported work;[19,21] (b) the average functionality for the monomer used in the experiment (one-functionality 2-EHA and two-functionality $PTPTP_n$) is evidently smaller than that used in the reported work (three-functionality TMPTA and two-functionality RM257).[19] Generally, monomers with lower functionality lead to lower crosslinking density and weaker anchoring energy of the polymer, which will beneficial to decreasing the saturation electric field (E_S) of the material;[34,35] (c) the helical twisting power (HTP) of the chiral agent (R811) used here is approximately 1/3 of that used in the reported work (ZLI-4572) (R811: HTP = 11.8 μm^{-1}; ZLI-4572: HTP = 34.2 μm^{-1}).[36] So it can be estimated that the pitch (P) of the sample is larger than those reported elsewhere. Therefore, according to eqn (6), larger $\Delta\varepsilon$, lower E_S, and smaller P will lead to a larger Kerr constant.

Fig. 12 also shows that the Kerr constant linearly increases from 10.1 nm V^{-2} (0.75 wt% dye) to 11.6 nm V^{-2} (1.75 wt% dye), with the increasing of dye content. The reason can be discussed through eqn (6) as well. The P in eqn (6) is constant; E_S is almost invariable according to the voltage-dependent CR curve shown in Fig. 6. Therefore, it can be deduced that Δn increases with the doping of the dye, which is the main reason for the increasing of K. To prove this deduction, we analyze the Δn of the dichroic dye theoretically. Generally, Δn is proportional to the ratio of molecular length (L) and width (D), that is $\Delta n \propto L/D$.[37,38] It is difficult to measure L and D directly, however, our previous studies show that calculating chemistry methods may be an effective way. Semi-empirical quantum chemistry algorithm, AM1, is used herein to obtain the optimal geometrical structure of the molecules,[39,40] and then L and D can be estimated. L and D for the NLCs host are calculated. The main component of the NLC host is 5CB (~60 wt%), so that the properties of the NLC host can be considered as similar to 5CB, thus for simplicity we only calculate the ratio of 5CB here. Fig. 1(b) and (c) give the atomistic models for the optimal geometrical structures of 5CB and the dichroic dye, respectively. The length and width of 5CB are 15.36 Å and 5.10 Å; and those of the dye are 25.69 Å and 4.50 Å. Thus L/D is about 3.0 for 5CB, while the ratio for the dye is larger, about 5.7. In addition, analyzing from the single-band model of birefringence,[41,42]

$$\Delta n = G\frac{\lambda^2\lambda^{*2}}{\lambda^2 - \lambda^{*2}} \quad (7)$$

the parameter G is a constant related with alignment and packing of molecules; λ^* is defined as the mean electronic transition wavelength, which is proportional to the conjugation

length of the molecule; λ is the wavelength of the light source. From the chemical structure viewpoint, λ^* of the dye is larger than that of the NLC host due to the longer conjugation length. Therefore, combining the L/D ratio with the single-band model, Δn of the dye is deduced to be larger than that of the NLCs. Actually, our experiment also confirms the above deduction. The birefringence of the NLCs doped with 1.75 wt% dyes is about 0.003 larger than that of NLCs without dyes. Hence, doping the dye into the CLC system will inevitably raise the electric-field-induced birefringence, and thus increase the Kerr constant of the sample. The linear relationship between Kerr constant and dye content is attributed to the linear relationship between the birefringence and the dye content.[43]

In addition, comparing with the previous reported dichroic dye-doped PSBP,[22] the dichroic dye-doped PS-OICLC has several significant merits: (a) the saturation electric field (E_S) for PS-OICLC is lower. As reported, E_S of the dye-doped PSBP is $\sim$13 V μm^{-1}, which is much larger than that of the dye-doped PS-OICLC, $\sim$5 V μm^{-1}. The reason is mainly related to the large $\Delta\varepsilon$ (33.3) of NLCs we used, which is twice as large as that of 5CB (the NLC host used in the reported work to form PSBP, $\Delta\varepsilon = 11.5$); (b) the response time of dye-doped PS-OICLC is hundreds of microseconds, while that of dye-doped PSBP is several milliseconds, because of the two-step response; (c) the CR is improved from the reported 3.23 to 8.9, because of the high dichroism dye doped in the system. This value is lower than that of conventional PS-OICLC displays,[44] since there is no polarizer in the dichroic dye-doped PS-OICLC display. However, if the reflection mode is adopted, according to eqn (3), CR will increases to the square of that in transmission mode, $(8.9)^2 \approx 80$, which will satisfy the requirement for video applications;[30] and (d) the working temperature range of the PS-OICLC is large, and the structure is very stable even the temperature is below 0 °C, however we find the reported PSBP only works in the range from 20 to 40 °C. Thus, from the application viewpoint, the dye-doped PS-OICLC is more suitable.

Conclusions

In conclusion, the dichroic dye-doped PS-OICLC has been studied. The experimental results indicate that this material is very stable in a large temperature range and has many excellent properties for display technology, such as polarization -independence, sub-millisecond response time and high Kerr constant. The contrast ratio is 8.9, which is also several times larger than that of dye-doped PSBP material, and it can be increased to about 80 if the reflection mode is adopted. Improving the dichroism, the solubility and the order parameter of the dye, or extending the optical path, can increase the contrast ratio further. In addition, doping with a high birefringence dye can increase the electric-field-induced birefringence, and thus improve the Kerr effect of the material. We consider this kind of material will save at least 50% power consumption in applications, due to its polarization independence and fast response time. Therefore, such a material is promising for electronic tags, books, billboards, or optical filters and other photonic devices.

Acknowledgements

This work is sponsored by the National Science Foundation of China (no. 61108065) and the Chen-guang Talent Foundation of Shanghai Education and Development Committee (no. 12CG32). The authors also want to express their gratitude for great support from Infovision Optoelectronics Co., Ltd.

Notes and references

1 J. Yan, L. Rao, M. Jiao, Y. Li, H. C. Cheng and S. T. Wu, *J. Mater. Chem.*, 2011, **21**, 7870.
2 H. Kikuchi, *Struct. Bonding*, 2008, **128**, 99.
3 D. C. Wright and N. D. Mermin, *Rev. Mod. Phys.*, 1989, **61**, 385.
4 H. Kikuchi, M. Yokota, Y. Hisakado, H. Yang and T. Kajiyama, *Nat. Mater.*, 2002, **1**, 64.
5 H. J. Coles and M. N. Pivnenko, *Nature*, 2005, **436**, 997.
6 A. Yoshizawa, M. Sato and J. Rokunohe, *J. Mater. Chem.*, 2005, **15**, 3285.
7 Z. Zheng, D. Shen and P. Huang, *New J. Phys.*, 2010, **12**, 113018.
8 H. Yoshida, Y. Tanaka, K. Kawamoto, H. Kubo, T. Tsuda, A. Fujii, S. Kuwabata, H. Kikuchi and M. Ozaki, *Appl. Phys. Express*, 2009, **2**, 121501.
9 L. Rao, J. Yan, S. T. Wu, S. Yamamoto and Y. Haseba, *Appl. Phys. Lett.*, 2011, **98**, 081109.
10 Y. Chen, J. Yan, J. Sun, S. T. Wu, X. Liang, S. H. Liu, P. J. Hsieh, K. L. Cheng and J. W. Shiu, *Appl. Phys. Lett.*, 2011, **99**, 201105.
11 M. Wittig, N. Tanaka, D. Wilkes, M. Bremer, D. Pauluth, J. Canisius, A. Yeh, R. Yan, K. Skjonnemand and M. Klasen-Memmer, *Dig. Tech. Pap. - Soc. Inf. Disp. Int. Symp.*, 2012, **43**, 25.
12 J. Yan, Z. Luo, S. T. Wu, J. W. Shiu, Y. C. Lai, K. L. Cheng, S. H. Liu, P. J. Hsieh and Y. C. Tsai, *Appl. Phys. Lett.*, 2013, **102**, 011113.
13 Z. Ge, S. Gauza, M. Jiao, H. Xianyu and S. T. Wu, *Appl. Phys. Lett.*, 2009, **94**, 101104.
14 J. Yan, S. T. Wu, K. L. Cheng and J. W. Shiu, *Appl. Phys. Lett.*, 2013, **102**, 081102.
15 J. Yan, Y. Li and S. T. Wu, *Opt. Lett.*, 2011, **36**, 1404.
16 Y. Li and S. T. Wu, *Opt. Express*, 2011, **19**, 8045.
17 Y. H. Lin, H. S. Chen, H. C. Lin, Y. S. Tsou, H. K. Hsu and W. Y. Li, *Appl. Phys. Lett.*, 2010, **96**, 113505.
18 G. Zhu, J. N. Li, X. W. Lin, H. F. Wang, W. Hu, Z. G. Zheng, H. Q. Cui, D. Shen and Y. Q. Lu, *J. Soc. Inf. Disp.*, 2012, **20**, 341.
19 Y. Haseba, H. Kikuchi, T. Nagamura and T. Kajiyama, *Adv. Mater.*, 2005, **17**, 2311.
20 S. I. Yamamotoa, T. Iwatab, Y. Haseba, D. U. Choc, S. W. Choic, H. Higuchid and H. Kikuchid, *Liq. Cryst.*, 2012, **39**, 487.
21 Y. Haseba and H. Kikuchi, *Mol. Cryst. Liq. Cryst.*, 2007, **470**, 1.
22 Y. H. Lin, H.-S. Chen, T.-H. Chiang, C.-H. Wu and H.-K. Hsu, *Opt. Express*, 2011, **19**, 2556.

23 Z. Zheng, H. F. Wang, G. Zhu, X. W. Lin, J. N. Lin, W. Hu, H. Q. Cui, D. Shen and Y. Q. Lu, *J. Soc. Inf. Disp.*, 2012, **20**, 326.
24 Z. Zheng, W. Hu, G. Zhu, M. Su, D. Shen and Y. Q. Lu, *Chin. Opt. Lett.*, 2013, **11**, 011601.
25 J. Yan, H. C. Cheng, S. Gauza, Y. Li, M. Jiao, L. Rao and S. T. Wu, *Appl. Phys. Lett.*, 2010, **96**, 071105.
26 J. Yan, M. Z. Jiao, L. H. Rao and S. T. Wu, *Opt. Express*, 2010, **18**, 11450.
27 D. A. Skoog, D. M. West, F. James Holler and S. R. Crouch. *Fundamentals of Analytical Chemistry*, Thomson Learning Inc., Glendale, 2004.
28 K. M. Chen, S. Gauza, H. Xianyu and S. T. Wu, *J. Disp. Technol.*, 2010, **6**, 318.
29 C. Y. Fan, H. C. Jau, T. H. Lin, F. C. Yu, T. H. Huang, C. Liu and N. Sugiura, *J. Disp. Technol.*, 2011, **7**, 615.
30 S. T. Wu and D. K. Yang, *Reflective Liquid Crystal Displays*, John Wiley & Sons Ltd., 2001.
31 P. R. Gerber, *Mol. Cryst. Liq. Cryst.*, 1985, **116**, 197.
32 L. Rao, J. Yan and S. T. Wu, *J. Soc. Inf. Disp.*, 2010, **18**, 954.
33 L. Wang, W. He, X. Xiao, M. Wang, M. Wang, P. Y. Yang, Z. J. Zhou, H. Yang, H. F. Yu and Y. F. Lu, *J. Mater. Chem.*, 2012, **22**, 19629.
34 M. P. Stevens, *Polymer Chemistry*, Oxford University Press, 2nd edn, 1990.
35 R. T. Pogue, L. V. Natarajan, S. A. Siwecki, V. P. Tondiglia, R. L. Sutherland and T. J. Bunning, *Polymer*, 2000, **41**, 733.
36 *Liquid Crystal Device Handbook*, edited by Japan Society for Promotion of Science, the 142th Committee, Nikkan Kogyo Shimbun Ltd. Publish, 1989.
37 P. G. De Gennes and J. Prost, *The Physics of Liquid Crystals*, Clarendon, Oxford, 1993.
38 S. W. Choi, S. I. Yamamoto, Y. Haseba, H. Higuchi and H. Kikuchi, *Appl. Phys. Lett.*, 2008, **92**, 043119.
39 Z. Zheng, J. Ma, Y. Liu and L. Xuan, *J. Phys. D: Appl. Phys.*, 2008, **41**, 235302.
40 D. L. Cheung, S. J. Clark and M. R. Wilson, *Chem. Phys. Lett.*, 2002, **356**, 140.
41 D. K. Yang and S. T. Wu, *Fundamentals of Liquid Crystal Devices*, John Wiley & Sons Ltd., 2006.
42 S. T. Wu, *Phys. Rev. A*, 1986, **33**, 1270.
43 M. R. Fisch and S. Kumar, *Liquid Crystals: Experimental Study of Physical Properties and Phase Transitions*, Cambridge University Press, 2001.
44 S. W. Choi, S. I. Yamamoto, T. Iwata and H. Kikuchi, *J. Phys. D: Appl. Phys.*, 2009, **42**, 112002.

